Monatshefte für Chemie 137, 1119–1125 (2006)
DOI 10.1007/s00706-006-0521-1

Monatshefte für Chemie
Chemical Monthly
Printed in Austria

Structure and Magnetic Properties of Nickel–Zinc Ferrite Nanoparticles Prepared by Glass Crystallization Method

Ahmed M. El-Sayed[1,*] and **Esmat M. A. Hamzawy**[2]

[1] Inorganic Chemistry Department, National Research Centre, Dokki, Cairo, Egypt
[2] Glass Research Department, National Research Centre, Dokki, Cairo, Egypt

Received December 29, 2005; accepted (revised) March 2, 2006
Published online September 8, 2006

Summary. The magnetic and microstructure properties of Fe_2O_3–0.4NiO–0.6ZnO–B_2O_3 glass system, which was subjected to heat treatment in order to induce a magnetic crystalline phase ($Ni_{0.4}Zn_{0.6}$-Fe_2O_4 crystals) within the glass matrix, were investigated. DSC measurement was performed to reveal the crystallization temperature of the prepared glass sample. The obtained samples, produced by heat treatment at 765°C for various times (1, 1.5, 2, and 3 h), were characterized by X-ray diffraction, IR spectra, transmission electron microscopy, and vibrating sample magnetometer. The results indicated the formation of spinel Ni–Zn ferrite in the glass matrix. Particles of the ferrite with sizes ranging from 28 to 120 nm depending on the sintering time were observed. The coercivity values for different heat-treatment samples were found to be in the range from 15.2 to 100 Oe. The combination of zinc content and sintering times leads to samples with saturation magnetization ranging from 12.25 to 17.82 emu/g.

Keywords. Ni–Zn Ferrite; Nanoparticles; Borate glass matrix; Magnetic properties.

Introduction

Research interest in nanocrystalline materials and in granular magnetic solids consisting of ultra-fine or nanosized particles embedded in an immiscible insulating or metallic matrix has grown considerably in recent years due to new physical properties presented by these peculiar structures [1]. Giant magnetic coercivity has been observed in the case of nanosized iron particles having sizes in the range 2–10 nm and dispersed in an insulating matrix such as SiO_2 or Al_2O_3 [2, 3]. The coercivity reported is two orders of magnitude higher than that of bulk iron. This results from reduced sizes and effects of magnetic interactions among particles [4]. Soft ferrites having nanometer dimensions exhibit a much higher magnetic coercivity than samples having grain sizes of the order of few microns [5]. Nickel–zinc ferrites are magnetic materials that are much used by the modern electronics industry. This is

* Corresponding author. E-mail: ahmed_elsayed_3@hotmail.com

primarily due to their high electrical resistivity, which implies low eddy-current losses that become significant at higher frequencies of electromagnetic fields. Nickel–zinc ferrites also exhibit high values of magnetic permeability, *Curie* temperature, and dielectric constant, together with high mechanical strength, good chemical stability, and low coercivities [6]. The chemical precipitation method has been exploited in recent years to synthesize different ferrite particles having dimensions in the nanometer range, *e.g.* $CoFe_2O_4$ [7] and $Mn_{0.5}Zn_{0.5}Fe_2O_4$ [8]. The sol–gel technique has been utilized to prepare composites comprising of nanoparticles of iron [9] and $Ni_{0.5}Zn_{0.5}Fe_2O_4$ [10] in silica glass matrix. Previously in our laboratory *El-Sayed* [11–13] studied the effect of zinc content and chromium substitution on the structure and properties of nickel–zinc ferrites prepared by the usual ceramic method. Glass ceramics are consisting of a crystalline phase grown within a glass matrix. The aim of the present work is to prepare nickel–zinc ferrite ($Ni_{0.4}Zn_{0.6}Fe_2O_4$) particles of nanoscale dimensions within a borate glass matrix by glass-ceramic method and investigate the effect of heat-treatment on its structure and magnetic properties.

Results and Discussion

The XRD patterns of the glass sample sintered at 765°C for various sintering times in static air atmosphere are shown in Fig. 1. It is evident that in all cases only single

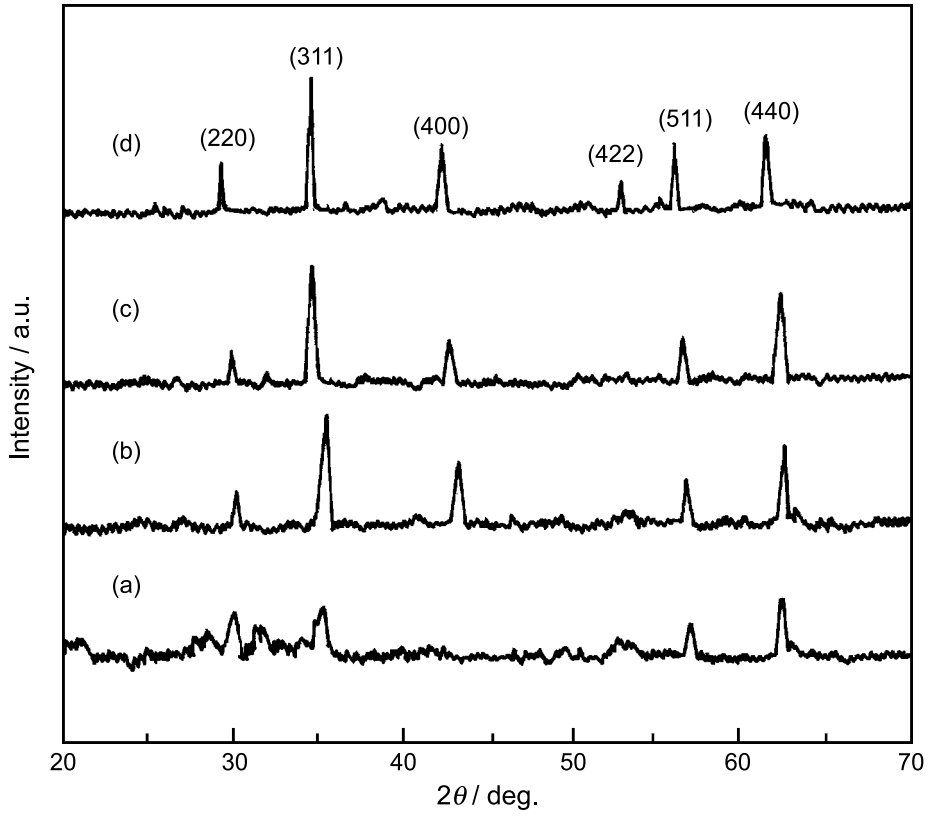

Fig. 1. XRD patterns of the glass sample sintered at 765°C for various times; (a) 1 h, (b) 1.5 h, (c) 2 h, and (d) 3 h

Table 1. The obtained data of the glass-ceramic samples containing $Ni_{0.4}Zn_{0.6}Fe_2O_4$

Sample no.	Heat treatment schedule	Lattice parameter Å	Particle size nm	*Hc* Oe	*Ms* emu/g
1	765°C for 1 h	8.356	28	100	15.25
2	765°C for 1.5 h	8.369	47	41.2	17.48
3	765°C for 2 h	8.373	62	16.5	17.65
4	765°C for 3 h	8.387	120	15.2	17.82

spinel phase is present. The relative intensities of the peaks show inverse spinel phase [14]. The formation of nickel–zinc ferrite is confirmed in all samples with no additional peaks corresponding to extra phases such as α-Fe_2O_3 being present in any of them which often appear when the reaction is not complete. The Ni–Zn ferrite system has a cubic spinel configuration with unit cell consisting of eight formula units of the form $(Zn_xFe_{1-x})[Ni_{1-x}Fe_{1+x}]O_4$ [15]. Thus, in the present investigation the distribution of cations in the two spinel sites is given by $(Zn_{0.6}Fe_{0.4})[Ni_{0.4}Fe_{1.6}]O_4$. Particle size of Ni–Zn ferrite phase in different samples was calculated from the area and full width of half maximum of (311) diffraction peaks using the software Topas 2 equipped with XRD and is shown in Table 1. It is evident that the lattice parameter and crystallite size of the ferrite phase vary from 8.356 to 8.387 Å and from 28 to 120 nm, respectively, depending on heat treatment schedule applied to the glass sample. The phase analysis performed on the samples after each treatment revealed the development of the Ni–Zn ferrite crystals in the glass matrix beginning with the sintering for 1 h. Because at this time the crystallites are very small, the X-ray peaks are weak [16]. The difference between the various crystallization times arises because the longer treatment time favors the formation of homogeneous temperature distribution within the glass matrix.

The transmission electron microscopy was used to view and record the microstructure of nanosized ferrite samples. TEM micrographs of the glass sample

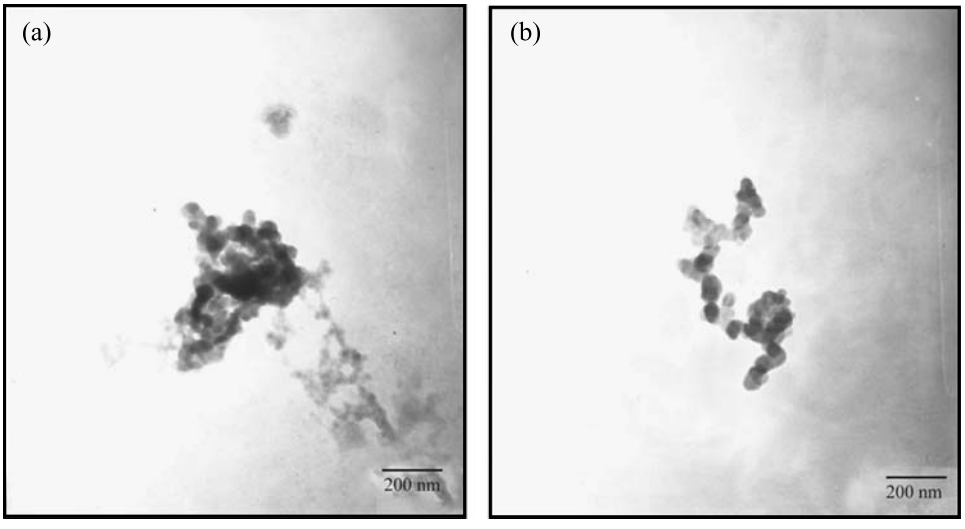

Fig. 2. TEM micrographs of the glass-ceramic samples sintered at 765°C for (a) 1 h and (b) 2 h

sintered at 765°C for 1 and 2 h are shown in Fig. 2. It can be seen that the agglomerates comprise relatively uniform-sized spherical particles. The average of particle sizes seems to be higher than that derived from XRD measurements. This is probably a result of the agglomeration of nanosized particles.

The IR spectra of the prepared samples were recorded to confirm the formation of Ni–Zn ferrite phase and to understand the nature of the glass matrix. The spectra are recorded at room temperature in the range from 400 up to 2000 cm^{-1}, Fig. 3. The samples show characteristic absorptions of Ni–Zn ferrite phase, the absorptions at 550 cm^{-1} and around 415 cm^{-1}, which confirm the formation of the Ni–Zn ferrite spinel phase in these samples [11, 12]. The characteristic bands of borate glass bonds around 700, 1000, and 1500 cm^{-1} are displayed in these samples. As mentioned in previous work [17–20] the incorporation of boron modifies the IR spectra into three groups of bands: a) The bands ranging from 1200–1600 cm^{-1} due to the asymmetric stretching vibration of B–O bond of trigonal BO_3 units, b) the next one range from 800–1200 cm^{-1} is due to the B–O bond stretching of the tetrahedral BO_4 units and c) the third group lies around 700 cm^{-1} due to bending of B–O–B linkage in borate network. Thus, the bands observed at 1440 and 1192 cm^{-1} are attributed to B–O or the trigonal units, whereas the bands at 1003, 897 and 798 cm^{-1} are assigned to the B–O bond stretching of the tetrahedral BO_4 units. Other bands at 723 and 636 cm^{-1} are assigned to bending of B–O–B linkages in borate network.

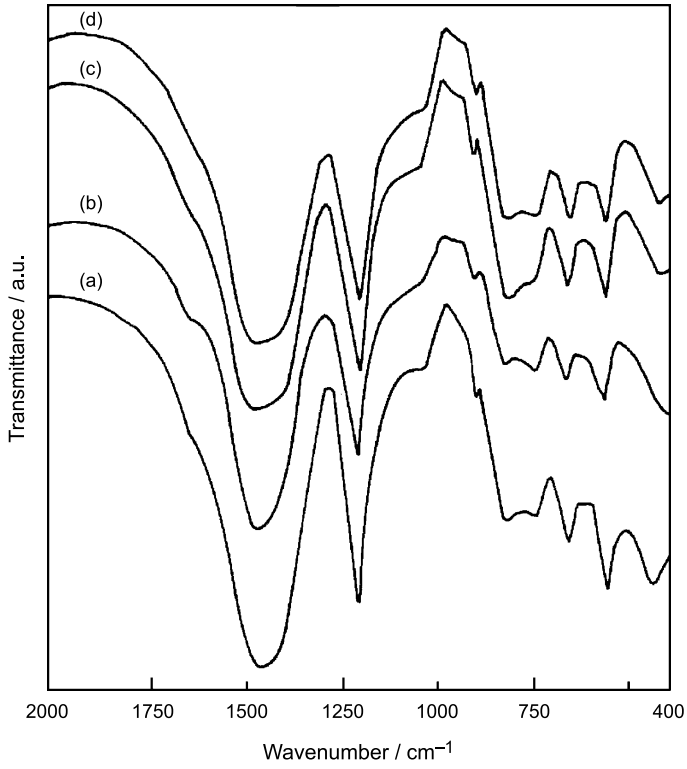

Fig. 3. IR spectra of the glass-ceramic samples sintered at 765°C for various times; (a) 1 h, (b) 1.5 h, (c) 2 h, and (d) 3 h

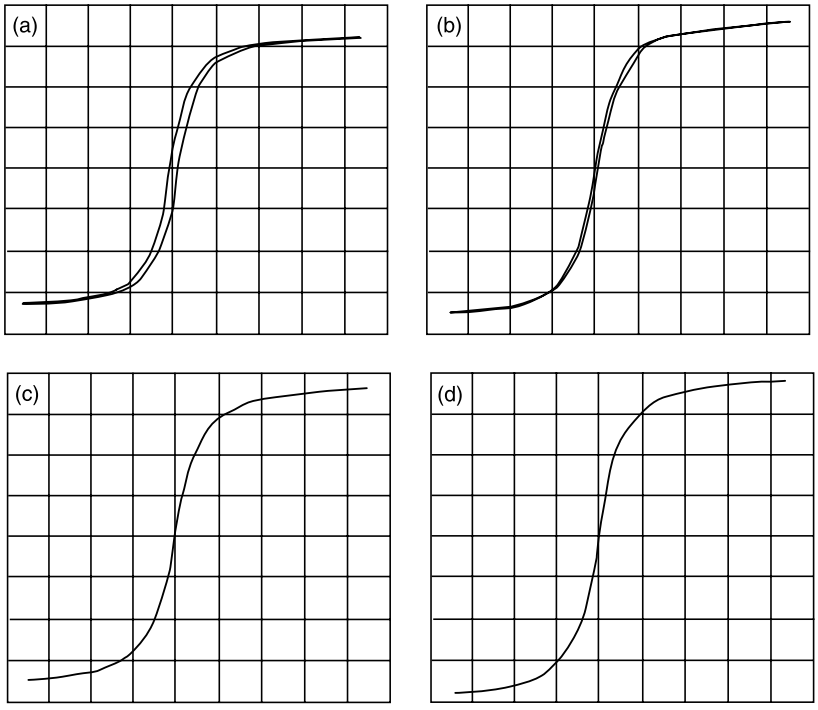

Fig. 4. Hysteresis loops of the glass-ceramic samples sintered at 760°C for various times (x: 1250 Oe/Div; y: 5 emu/g/Div)

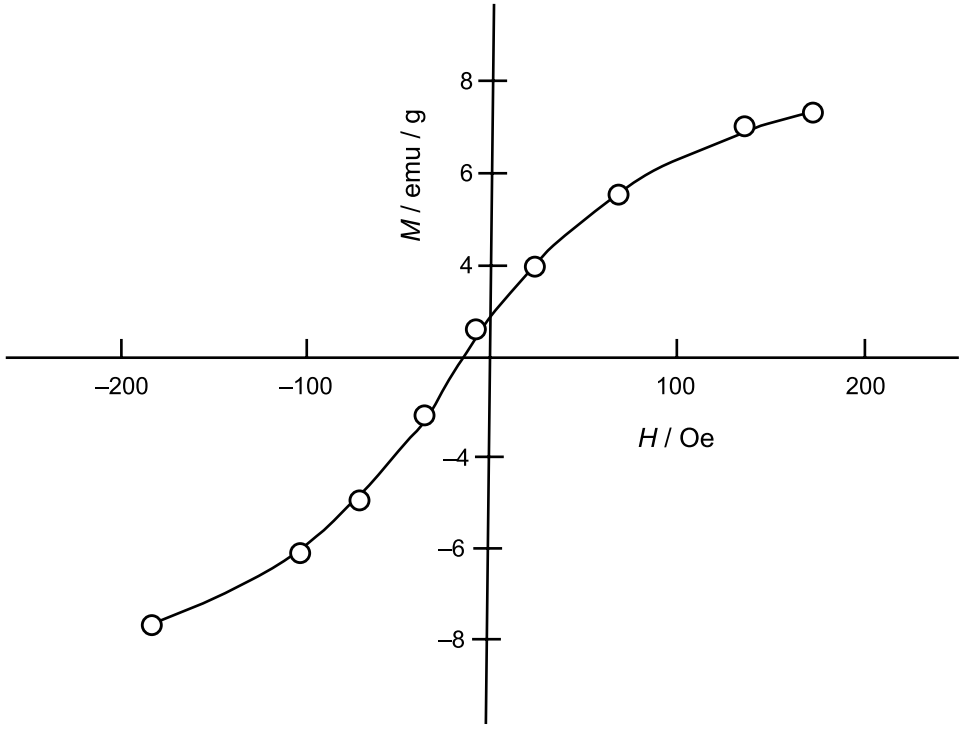

Fig. 5. Magnified plot of magnetization *vs*. magnetic field for sample 3

Figure 4 shows hysteresis loops of glass-ceramic samples sintered at 760°C for various times. In Fig. 5 the magnetization *versus* magnetic field plot for sample 3 (2 h) has been expanded over a limited range to show the coercive field. The coercivity of a fine particle material is one of its most significant parameters; this gives information on the magnetic state and on the quality of the material [21]. Table 1 summarizes the values of saturation magnetization (*Ms*) and coercivity (*Hc*) for the different samples. The coercivity values in these samples range from 15.2 to 100 Oe. The obtained values are higher than those measured at room temperature for $Ni_{0.5}Zn_{0.5}Fe_2O_4$ nanoparticles [5]. The maximum value of *Hc* was obtained in the case of sample 1, which has a particle size of 28 nm, and then it was found to decrease sharply. The decrease in *Hc* above 28 nm can be interpreted in terms of magnetic multidomaim structure. The small size particles are single-domain structures and thus the rotational magnetization mechanism is present. For higher particle sizes, the crystallites change into the multidomain state when the magnetization process is produced by the wall displacement which requires a smaller energy [16]. The saturation magnetization increases from 15.25 to 17.82 emu/g with increasing sintering time from 1 to 3 h, Table 1. This indicates that the sample with higher particle size induces a higher magnetization. This may be as a result of the improved crystallinity, which implies a better exchange interaction, when one can suppose that the whole amount of Ni–Zn ferrite was crystallized within the glassy host.

Conclusion

Nanocrystalline Ni–Zn ferrite, $Ni_{0.4}Zn_{0.6}Fe_2O_4$, in borate glass matrix was prepared by glass-ceramic method followed by heat-treatment at 765°C for various times (1–3 h). The prepared samples showed only inverse spinel phase in the XRD patterns. The crystallinity of the spinel phase was found to improve with the sintering time. IR spectra confirmed the formation of the spinel Ni–Zn ferrite phase within the borate glass matrix. Samples with Ni–Zn ferrite having particle dimensions in the range 28–120 nm were obtained. With increasing the sintering time the particle size and saturation magnetization were found to increase while the coercivity decreases. The above results suggest that the microstructure and magnetic properties of Ni–Zn ferrite in glass matrix can be controlled by correctly selecting the heat treatment.

Experimental

The glass composition chosen after a few trial runs was 8NiO (99.5% pure, BDH), 12ZnO (99.5% pure, BDH), $20Fe_2O_3$ (99% pure, BDH), and $60B_2O_3$ (99.5% pure, S.D. Fine-Chem. Ltd) in mol%. The starting materials were used in oxide form; B_2O_3 was introduced as H_3BO_3. The well mixed oxides for preparing about a 25 g batch were placed in an alumina crucible and melted in an electrically heated furnace at a temperature of ~1350°C for 2 h. The glass was prepared by pouring the melt onto an iced cooled brass plate. Another cooled brass plate was pressed on the molten mass to bring about quenching. The glass prepared as above was ground in a mortar and pestle. The crystallization temperature of the glass sample was determined using a SETARAM (Labsys^{TM} TG-DTA 16 model), heating rate 10°C/min. Figure 6 shows an exothermic peak at 765°C which is attributed to the crystallization of the prepared glass sample. On the basis of this result, the glass powder was subjected to heat-treatment at 765°C, in static air atmosphere, for various times (1, 1.5, 2, and 3 h) followed by natural furnace cooling to room temperature. Nickel–zinc ferrite was precipitated within the glass during this treatment. The prepared samples were investigated by X-ray diffraction (XRD) at room

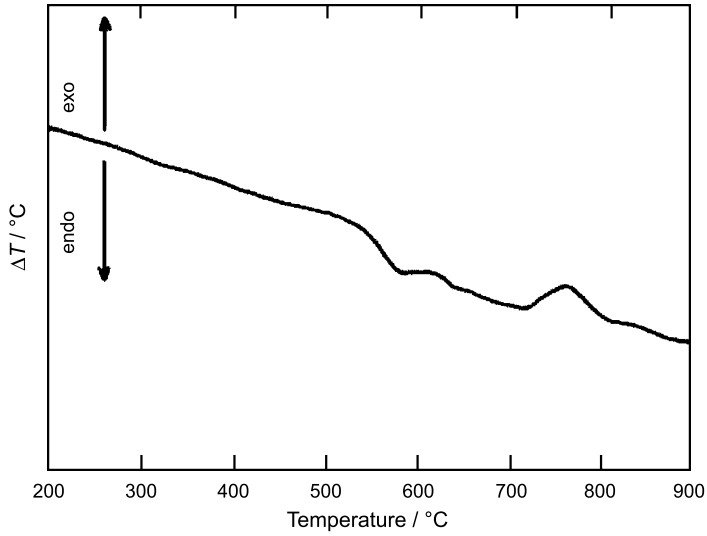

Fig. 6. DTA plot of the prepared glass sample

temperature using a diffractometer (model-Bruker AXS D8 advance) with Cu K_α radiation and a secondary monochromator. The IR spectra were recorded over the range 400–2000 cm^{-1} using a FTIR spectrometer (Nexus 670). The microstructure of the glass-ceramic samples was studied using a transmission electron microscope (Zeiss TEM-10). The samples for TEM analysis were dispersed in distilled water and then applied to a copper grid, where they were allowed to dry and latter viewed on the TEM. Magnetic measurements on the different samples were performed at room temperature using a vibrating sample magnetometer (VSM-Model 9600; accuracy ± 0.001).

References

[1] Albuquerque AS, Ardisson JD, Macedo WAA (1999) J Magn Magn Mater **192**: 277
[2] Gang X, Chien CL (1987) Appl Phys Lett **51**: 1280
[3] Liou SH, Chien CL (1988) Appl Phys Lett **52**: 512
[4] Rezlescu N, Rezlescu L, Craus ML, Rezlescu E (1999) J Magn Magn Mater **196**: 463
[5] Pal M, Brahma P, Chakravorty D, Bhattacharyya D, Maiti HS (1996) J Magn Magn Mater **164**: 256
[6] Uskokovic V, Drofenik M, Ban I (2004) J Magn Magn Mater **284**: 294
[7] Haned K, Morris AH (1988) J Appl Phys **63**: 4258
[8] Pannaparayil E, Marande R, Komarneni S (1991) J Appl Phys **69**: 5349
[9] Chatterjee A, Das D, Chakravortty D, Choudhury K (1990) Appl Phys Lett **57**: 1360
[10] Chatterjee A, Das D, Pradhan SK, Chakravorty D (1993) J Magn Magn Mater **127**: 214
[11] El-Sayed AM (2002) Ceram International **28**: 363
[12] El-Sayed AM (2002) Ceram International **28**: 651
[13] El-Sayed AM (2003) Mater Chem Phys **82**: 583
[14] Sankaranarayanan VK, Sreekumar C (2003) Current Appl Phys **3**: 205
[15] Jacobo SE, Duhalde S, Bertorello HR (2004) J Magn Magn Mater **272–276**: 2253
[16] Rezlescu N, Rezlescu E, Pasnicu C, Craus ML (1994) J Magn Magn Mater **131**: 273
[17] Wong J, Angell CA (1976) "Glass/Structure by Spectroscopy" New York, Basel: Dekker, Ch. **7**
[18] Chakrabarty IN, Condrate RA (1986) J Non-Cryst Solids **81**: 271
[19] Julien C, Massot M, Balkanski M, Krol A, Nazarewicz W (1989) Mater Sci Eng **B3**: 307
[20] Chrssikos GD, Kamitsos EI, Karakassides MA (1990) Phys Chem Glasses **31**: 109
[21] Rezlescu N, Rezlescu E, Giobotaru I, Craus ML, Popa PD (1998) Ceram International **24**: 31